

CHAPTER 4

DATA ANALYSIS

The following sections elucidate many of the data analysis schemes that have been developed for use with the AVHT. However, most methods can be applied to the results of any tracking algorithm. Many *C* functions to assist in the data analysis are given in Appendix B under *stat.h*. Where appropriate, references to the relevant functions will be made in footnotes.

4.1 Track Origin Distributions

The process of examining tracks in the AVHT DST and comparing them to tracks from the GEANT DST reveals many tracks, especially heads, in the AVHT DST that do not appear in the GEANT DST. Fortunately, many of these spurious tracks have common features. Spurious heads usually have trajectories that do not approach the nominal collision point very closely. To determine the probability that a track originated from the nominal collision point, C0, a probability metric¹ similar to that employed in Section 3.5 is used:

$$P_{C_0}(\vec{p}, C_2, z) = P_{2D}(\sqrt{\vec{p} \cdot C_2^{-1} \cdot \vec{p}^t}) P_{1D}(z/17) \quad (4.1)$$

where \vec{p} is the 2-vector describing the (x,y) coordinates of the point where the track in question passes closest to the beam axis (PCA—point of closest approach), z is the z-coordinate of this point and C_2 is the 2x2 covariance matrix describing the errors in \vec{p} . The probability for the z-coordinate separates from the probability for the x- and y-coordinates in the probability distribution because the correlations between the z- and the x- and y- positions of the PCA are unknown; however, it is known that the standard deviation in the z-position of the collision vertex is approximately 17” about C0. Given a set of track parameters (3.4), the z-positions of the two relevant projective planes, (z_0, z_1) , and the covariance matrix, C , describing the errors in the track, the PCA, \vec{P} , can be computed by the following method.

¹ The function *stat.c:SourceProb* computes this probability for any given track using the covariance matrices (3.15). It returns the *S*-value of the probability.

With the introduction of the 3-vectors

$$\vec{x}_0 = (x_0, y_0, z_0), \quad (4.2a)$$

$$\vec{x}_1 = (x_1, y_1, z_1), \quad (4.2b)$$

$$\vec{b} = (0, 0, 1), \quad (4.2c)$$

$$\vec{u} = \frac{\vec{x}_1 - \vec{x}_0}{|\vec{x}_1 - \vec{x}_0|}, \quad (4.3)$$

where the unit vector \vec{b} represents the direction of the proton beam, \vec{P} can be written as

$$\vec{P} = (\vec{p}, z) = \vec{x}_0 + \vec{u} \frac{(\vec{x}_0 \cdot \vec{u}) - (\vec{b} \cdot \vec{u})(\vec{b} \cdot \vec{x}_0)}{(\vec{b} \cdot \vec{u})^2 - 1}. \quad (4.4)$$

Propagation of errors yields the following formula for C_2

$$(C_2)_{ij} = \sum_{n=0}^3 \sum_{m=0}^3 \frac{\partial F_i}{\partial \vec{v}_n} \frac{\partial F_j}{\partial \vec{v}_m} C_{nm}, \quad (4.5)$$

where

$$\vec{v} = (x_0, y_0, x_1, y_1). \quad (4.6)$$

Here the F_i are given by (2.1) and are evaluated at the z-position of the PCA. The application of (4.1) separately to all heads found by the AVHT² and all heads present in the GEANT DST yields Fig. 4-1.

² With the application of the now standard *Chi-Squared* and *Same-Track Cuts*.

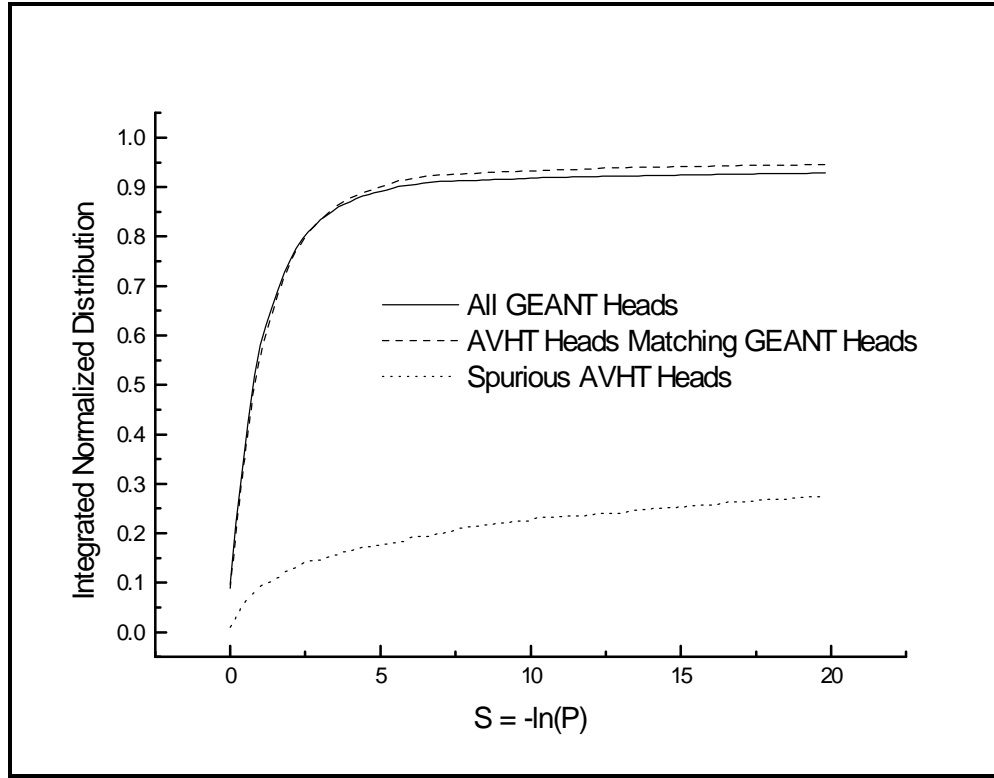


Fig. 4-1: Track Origin Distributions

Fig. 4-1 shows that real tracks from primary particles have an overwhelming probability of appearing to come from the nominal collision point. Other tracks (5% of the total and emanating from beam pipe conversions or other interactions and decays) show negligible probability for coming from C0. An examination of the corresponding distribution for AVHT tracks reveals the same effect; however the distribution for spurious AVHT tracks indicates that only about 20% of these seem to come from the vicinity of C0. It is evident that tracks from primary particles found by the AVHT show a probability of $S < 5$ of originating at C0. Making a SourceCut of $S = 5.0$ will have the effect of eliminating about 80% of the spurious tracks and will thus serve well in increasing the tracking efficiency. However, if information is desired about the few percent of tracks emanating from interactions before the detector, these should be detected before the *Source Cut* is applied. An interesting class of tracks, specifically those descended from the decay of certain neutral particles (such as K_S^0 and Λ^0), will also usually appear to originate from places far from C0. See Section 4.3 for suggestions on identifying these tracks. This cut is actually not performed by the AVHT so as to allow the analysis of the few percent of tracks originating from particles decaying or interacting; however, it should be applied at time of analysis.

4.2 Matching Heads and Tails

Chapters 2 and 3 and Section 4.1 establish how to find the heads and tails of tracks separately and also indicated how to control, somewhat, the spurious tracks also found. The next, and perhaps most important, task consists of fitting these two sets of tracks together to determine what really happened in the event. There will be several classes of track groups produced from this procedure: charged tracks passing through all MWPCs (1,1), charged tracks passing through only the front of the MWPCs (1,0) and charged tracks passing only through the back MWPCs (0,1). The (n,m) notation refers to the number of heads and tails, respectively, that contribute to the track. The first set of tracks are usually due to primary charged pions, though they can also be produced by the interaction of gammas in the Al window or by the decay of other particles. The second group consists mainly of two types of tracks. The first are tracks due to interactions in the beam pipe that are incident at such large angles so as to miss the PbC. The second are tracks that should have tails associated with them, but do not. These are probably mostly spurious. The final category of tracks consists of tracks due to particles created by interactions in the PbC or the beam pipe. In general, there is another category, (0,n), that refers to several charged tracks having a common vertex in the PbC. These are cases when multiple interaction products are detected.

It is necessary to determine, as efficiently as possible, the reason for the occurrence of each head and tail in the AVHT DST. The first step in this direction is to calculate the probability that two tracks have a common vertex in the PbC. The probability of coincidence of these two tracks³ can be computed via (3.33).

$$P_{same}(\vec{y} = \vec{x}_1 - \vec{x}_2, C_1, C_2) = P_{2D}(\sqrt{\vec{y} \cdot (C_1 + C_2)^{-1} \cdot \vec{y}'}) \quad (4.7)$$

where \vec{x}_1 and \vec{x}_2 are the 2-vector positions of the tracks at the PbC. The 2x2 covariance matrices represent the errors in the positions of these two points on the PbC. These tracks could be a head and a tail, two tails or even two heads. This method takes the different errors for heads and tails into account. For charged tracks passing through the entire detector, the head-to-tail matching is fairly easy. Fig. 4-2 shows that 97% of heads and tails from the same GEANT charged track have a probability of coincidence less than 6.0. Those with smaller probabilities have been seen to interact greatly in the PbC such that their trajectories are discontinuous. It can also be seen from Fig. 4-2 that only 3.2% of heads and tails from different charged tracks have a probability of coincidence less than 6.0. These mostly arise in higher multiplicity events when there are pairs of particles traveling fairly close together.

³ This probability is calculated by the function *stat.c:HeadTailProb*. Despite its name, it computes the probability of coincidence for head-tail or tail-tail.

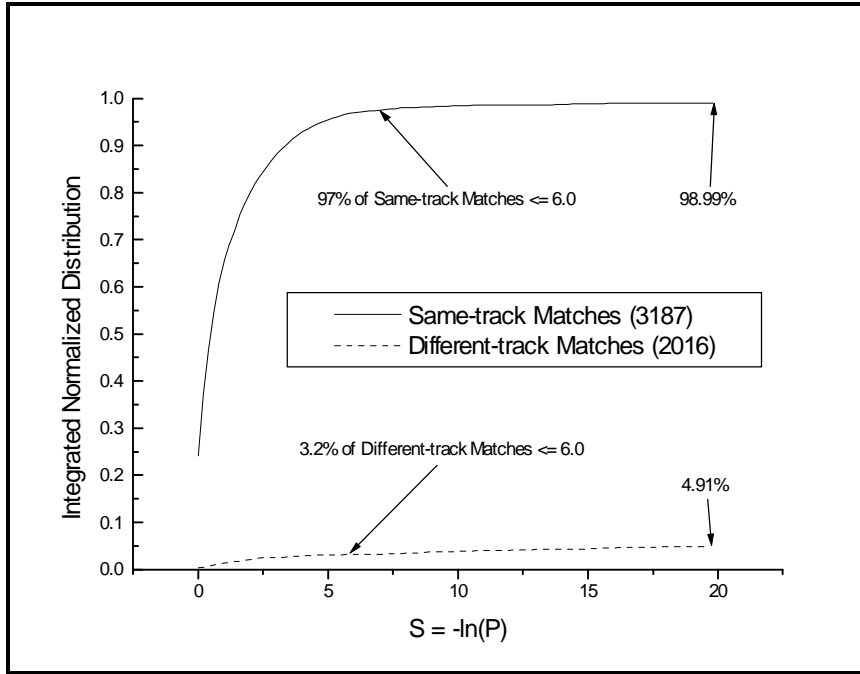


Fig. 4-2: Head-Tail Matching GEANT Tracks

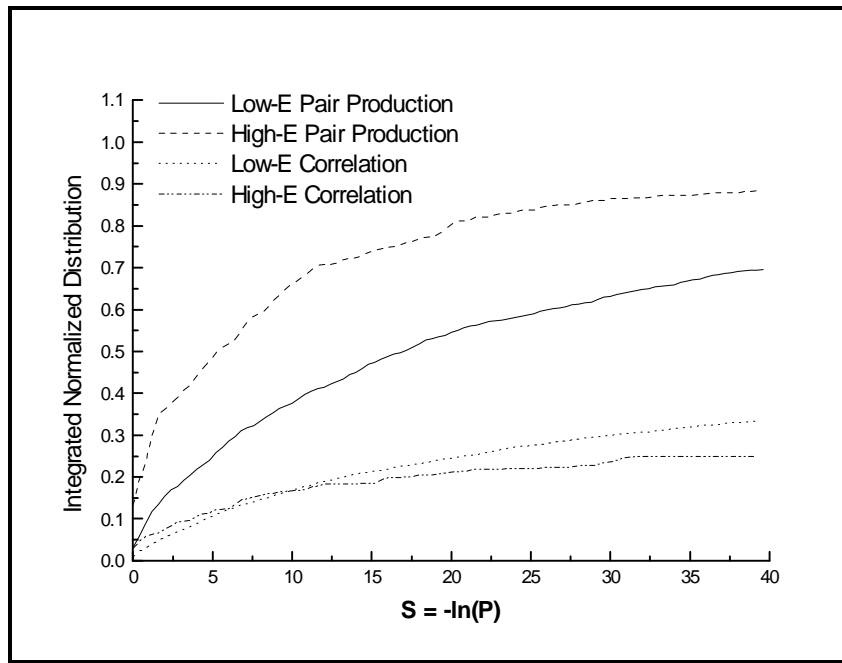


Fig. 4-3: Tail-Tail Matching GEANT Tracks

The information contained in Fig. 4-2 allows one to potentially match heads and tails coming from the same particle. However, it is more difficult to match multiple tails to a single vertex in the PbC. GEANT provides information about pairs of tracks resulting from pair production in the PbC. Applying (4.7) to these pairs yields an expected distribution of probabilities for matching. Two separate distributions were made. The high-energy distribution corresponds to those pairs of tracks where both particles had energy greater than 1 GeV. The low-energy distribution corresponds to all other pairs. It is clear that the high-energy pairs multiple scatter in the PbC less and thus point more definitely back to a common vertex. However, it is somewhat surprising how much multiple scattering affects even the high-energy tracks. As a comparison, the probability distribution for tails from different groups (e.g. different pairs or singlets) was also compiled and shown above in Fig. 4-3 as the correlations. Much of the early rise (about 15% of it) is due to contamination from multiple-particle showers that were not grouped together. The distributions for these correlations are almost flat after $S=6$ or so. So a grouping cut can be extended to a fairly large probability region without significant loss in resolution. This will cut down on the number of spurious neutral tracks identified. A preliminary cut of about $S=20$ seems reasonable since the high-energy distribution for pair production has about crested by this point. More detailed studies examining these distributions as functions of particle type and energy should be performed to fine tune this cut.

One way to combat the effects of multiple scattering in the identification of vertices in the PbC is to apply the procedures developed next in Section 4.3. It seems reasonable that while multiple scattering may deflect the trajectories of the particles enough so that they do not form a clear vertex on the PbC, they might still approximately form a vertex at a slightly different z-coordinate. In fact, the presence of multiple scattering makes information gained by tracing the tails back to a given plane much less useful. The possibility of using vertex information rather than probabilistic information for matching tails will be explored in the following section.

4.3 Two-Track Vertices

The ability to identify tracks originating from the same vertex is very useful for many purposes including the identification of electromagnetic shower vertices, the nominal collision point and particle decays. There are several methods for discerning two-track vertices. The simplest method, which provides a good quick check as to whether two tracks could possibly have a common vertex, involves determining the distance of closest approach (DCA) of the trajectories of the two tracks. This measure can be calculated analogously to (4.2) through (4.4). If the two track trajectories, x and x' , are parameterized by the usual set of two points each

$$\bar{x}_0 = (x_0, y_0, z_0), \quad (4.8a)$$

$$\bar{x}_1 = (x_1, y_1, z_1), \quad (4.8b)$$

$$\bar{x}'_0 = (x'_0, y'_0, z'_0), \quad (4.8c)$$

$$\bar{x}'_1 = (x'_1, y'_1, z'_1), \quad (4.8d)$$

and the vectors

$$\bar{u} = \frac{\bar{x}_1 - \bar{x}_0}{|\bar{x}_1 - \bar{x}_0|}, \quad (4.9a)$$

$$\bar{u}' = \frac{\bar{x}'_1 - \bar{x}'_0}{|\bar{x}'_1 - \bar{x}'_0|}, \quad (4.9b)$$

$$\bar{v} = \bar{x}'_0 - \bar{x}_0, \quad (4.9c)$$

are defined, then the DCA⁴, obtained by minimizing the distance between two lines, is

$$d = \left| \bar{u} \frac{-(\bar{u}' \cdot \bar{u})(\bar{u}' \cdot \bar{v}) + (\bar{v} \cdot \bar{u})}{1 - (\bar{u}' \cdot \bar{u})^2} - \bar{u}' \frac{-(\bar{v} \cdot \bar{u}') + (\bar{u}' \cdot \bar{u})(\bar{u} \cdot \bar{v})}{1 - (\bar{u}' \cdot \bar{u})^2} - \bar{v} \right|. \quad (4.10)$$

This gives a rough estimate of how close the two tracks approach each other. Another useful quantity also obtainable from the minimization problem is the vector position,⁵ \vec{V} , of the midpoint between the points of closest approach of the two tracks, essentially, the nominal vertex. This position is given by the formula

$$\vec{V} = \bar{p} + (\bar{p}' - \bar{p}) \cdot d, \quad (4.11a)$$

$$\bar{p} = \bar{u} \frac{-(\bar{u}' \cdot \bar{u})(\bar{u}' \cdot \bar{v}) + (\bar{v} \cdot \bar{u})}{1 - (\bar{u}' \cdot \bar{u})^2} + \bar{x}_0, \quad (4.11b)$$

$$\bar{p}' = \bar{u}' \frac{-(\bar{v} \cdot \bar{u}') + (\bar{u}' \cdot \bar{u})(\bar{u} \cdot \bar{v})}{1 - (\bar{u}' \cdot \bar{u})^2} + \bar{x}'_0, \quad (4.11c)$$

where \bar{p} and \bar{p}' are the points of closest approach on each track. If the DCA is too large or if the nominal position of the vertex is unreasonable then the two tracks are highly unlikely to originate from the same vertex. For small distances of closest approach, they probably do; however, a more precise method is needed to compute exactly how well they point back to the vertex, as well as to determine the actual vertex position. This involves a seven parameter nonlinear LSF—nonlinear because the exact z-position of the vertex is unknown.

⁴ This is computed by the functions *coords.c:vdDistance* and *stat.c:trkDCA*.

⁵ The functions *coords.c:vdMidPoint* and *stat.c:trkVertex* both compute this quantity.

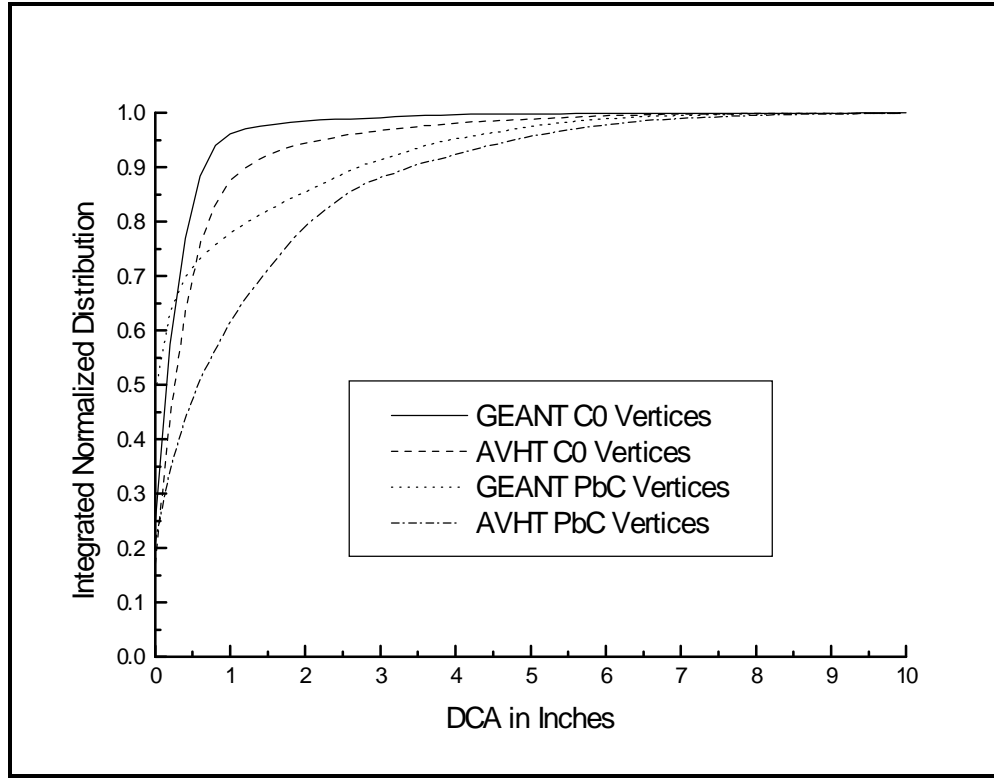


Fig. 4-4: Two-Track DCA's near C0 and the PbC

Fig. 4-4 shows the expected distribution of DCA's near C0 and the PbC for GEANT and AVHT tracks. Only track pairs whose nominal vertex was within a 100" long by 15" radius cylinder centered on C0 or within a 20" long by 10" radius cylinder centered around the PbC were kept. The large proportion of vertices show very small DCA's—under 1". Also, the AVHT curves are not very different from the respective GEANT curves, though the differences arise mostly from the presence of spurious tracks and the loss of other tracks in the AVHT. More informative distributions, similar in approach to Figs. 4-2 and 4-3, look at the DCA distributions for tracks that are known to have common vertices and tracks known not to have common vertices.

Fig. 4-5 displays the DCA distribution for pairs of GEANT heads and tails that are known to originate from the same vertex. As before, the multiple scattering in the PbC is evident from the shape of the curve for tails. Using the *Same-Track Cut* of 3.0 on the AVHT DST file to determine which AVHT tracks corresponded to which GEANT tracks allows one to make analogous distributions for AVHT tracks coming from the same vertex. These tracks, as shown in Fig. 4-5, tend to have a somewhat larger DCA than the GEANT. This is due to many factors inherent in the tracking scheme—for instance, if the actual track contains wires that could be eliminated in order to obtain a better χ_v^2 , then the AVHT will find the track without the extra wires, resulting in a track with a somewhat different trajectory.

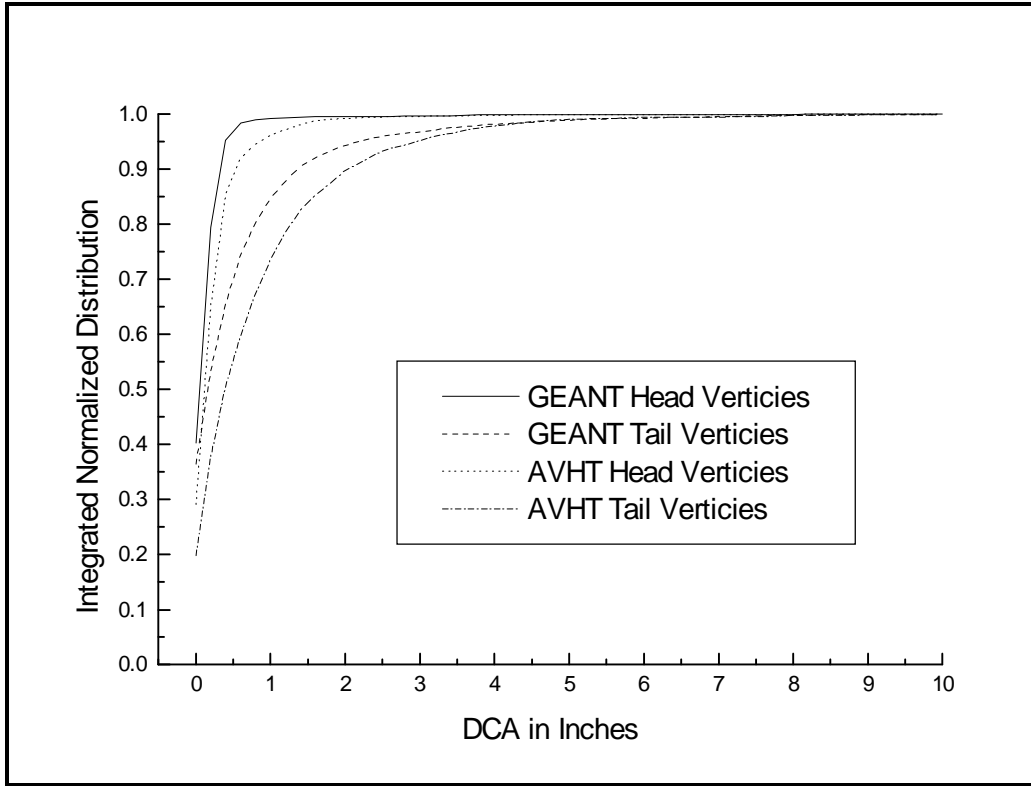


Fig. 4-5: DCA Distribution of Known Vertices

So, a DCA cutoff of one or two inches is large enough to catch most actual vertices; however, a DCA cutoff is not enough. Many tracks that do not originate from the same vertex also have small DCA's, although their nominal vertex is usually in a strange place. So by making cuts on the x-, y- and z-position of the nominal vertex, many spurious vertices can be eliminated.

Once candidate vertices passing appropriate DCA and nominal vertex cuts are in hand, one can perform a nonlinear LSF on the tracks, constraining them to a common vertex. While this has been done in the past, it is not currently implemented; however, the Levenberg-Marquardt method⁶ is recommended. It should be noted that while the nonlinear LSF provides very good means for dealing with vertices from heads, the multiple scattering prevalent in the tails makes the nonlinear LSF useless. This is because any fit will likely yield a vertex position very much different than the actual one. For examining tail vertices, some combination of the probabilistic method (4.7) and the DCA method should be employed.

⁶ Numerical Recipes in C, p 683.

4.4 Identifying Charged and Neutral Particles

The analysis of Chapter 3 and the preceding sections of this chapter can be summarized into a potential overall data analysis strategy. While the individual steps in the data analysis surely need more refinement, the following should provide a sound outline.

- I. Find all heads and tails in the event using any tracking scheme.
 - A. Use appropriate *Same-Track* and *Chi-Squared Cuts* to remove spurious tracks.
 - B. Do not make any *Source Cut* at this stage.

- II. Identify tracks from decay products, C0 or the beam pipe.
 - A. Examine all pairs of heads using DCA and nominal vertex information to determine if they could form a vertex.
 - B. Use a nonlinear LSF where appropriate to obtain more accurate vertex information.
 - C. Make a *Source Cut* on heads that do not contribute to a vertex in an acceptable region of space, e.g. near the beam or in the beam pipe.
 - D. If there are vertices within the pipe within $\pm 50''$ of C0 and fairly close to the beam, they can possibly determine the actual collision point, otherwise, C0 can be assumed.
 - E. Heads and head-vertices coming from near the pipe, but not directly from the collision point can be labeled as electromagnetic conversion products—the signature of a γ -conversion.

- III. Identify “charged particles.”
 - A. Match heads to tails as described in Section 4-2, looking for charged tracks passing through the entire detector.
 - B. Remember that these might not all be primary particles, so not all heads will have tails at this stage.

- IV. Identify interaction products from the PbC.
 - A. Use DCA and probabilistic methods to group tails together into sets of tracks coming from the same small volume in the PbC.
 - B. Many groups will only have one tail.
 - C. Each group probably represents one particle incident on the PbC.

- V. Group interaction products with heads.
 - A. If a member of the group of interaction products has already been identified with a head, then the whole group is.
 - B. Otherwise, use probabilistic or proximity methods to determine if any heads could have produced the observed interaction products.
 - C. The whole shower, including the head and the interaction products, can probably be attributed to an electron coming from the conversion

of a γ in the beam-pipe or window.

- VI. Remove other spurious tracks.
 - A. Heads without tails that point in a direction passing through the back acceptance of the detector are probably either spurious or very low-energy electrons emanating from the beam pipe, mostly the former. These should be removed.
 - B. It is arguable that so-far unaccounted for tails which do not point towards the collision point are either spurious or resulting from the beam pipe. These probably should also be removed.
 - C. Information from the electromagnetic calorimeters could be employed to help verify whether questionable tails are really valid.

- VII. Perform auxiliary data analysis.

Many of these steps have been analyzed in great detail here in this thesis; however, many still need much investigation. In particular, the best method for employing the probabilistic and DCA methods for determining tail-vertices is as yet unknown due to its difficulty. Also, the information delivered by the electromagnetic calorimeters is just beginning to be studied. In addition to the preceding procedure for determining the incident charged and neutral particles in an event, along with their subsequent interaction products, the relative efficiencies of the tracking and data analysis procedures described must be known if anything meaningful is to be said about the resultant data. This process is started in the following section, but is by no means complete.

4.5 Evaluation of Efficiencies and Systematic Errors

The AVHT DST file used in much of the above analysis was made with fairly loose cuts—a *Same-Track Cut* of 1.0 and a *Chi-Squared Cut* of 4.0 for both types of tracks. Originally, a DST file was made without any cuts; however, this type of file has proven to be ill-suited for the analysis of efficiencies. To understand why this is so, one must first remember how that AVHT handles the *MinPlanes Cut*. If there are N planes in the region of the detector being tracked, the AVHT will be applied first with a *MinPlanes Cut* of N . Then, all the wires from tracks found will be removed from the event and *MinPlanes* will be decremented and the procedure repeated. Under normal conditions, this process speeds up tracking by more than an order of magnitude while also eliminating many potential spurious tracks; however without cuts, very many tracks are found in the early stages of tracking. These tracks often contain wires belonging to real tracks that pass through fewer planes. So the process of deleting these wires from the event effectively eliminates the possibility of detecting certain real tracks. If even loose cuts are applied, the number of tracks found is sufficiently reduced by this process that this problem does not result in any statistically noticeable effect. Therefore, the DST file with loose cuts will be used in the following analysis.

Even the preceding loose cuts have already compromised some potential track-finding efficiency, especially in the detection of tracks with very similar trajectories and tracks with not very straight trajectories. The useful quantities in measuring efficiency are the percentage of incident tracks found, average number of spurious tracks found per event as a function of incident multiplicity. If the AVHT DST and the GEANT DST⁷ are compared and a *Same-Track Cut* of 3.0 is used to match AVHT to GEANT tracks and call them found, base-line efficiencies can be obtained for detecting the heads and tails actually present. It should be noted that only GEANT heads and tails passing the appropriate *MinPlanes Cut* were considered. This is not a major deficiency since GEANT assumes perfectly efficient wires and hence tracks not passing the *MinPlanes Cut* probably do not pass through the whole acceptance of the detector.

Incident Heads	Percent Found	Spurious per event		Incident Tails	Percent Found	Spurious per event
0		1.08		0		1.03
1	97.38+/-2.31	2.28		1	91.40+/-2.55	2.32
2	94.82+/-2.37	4.2		2	86.10+/-2.33	3.23
3	91.58+/-3.01	6.98		3	81.59+/-2.59	5.14
4	87.00+/-4.44	11.78		4	76.81+/-2.87	6.71
5	80.76+/-6.20	14.78		5	68.82+/-3.34	9.97

Table 4-6: Base-Line Efficiencies for Detecting Heads and Tails.

Table 4-6 displays the base-line efficiencies. The large numbers of spurious tracks present are not worrisome since much stronger cuts have yet to be applied. It is noticeable that while low multiplicity events have a fairly high efficiency, the higher occupancy ones do not. Going beyond 5 incident particles, the efficiencies are worse; however, the number of events in this region is too small to make the statistics meaningful. One effect the efficiency loss is displaying is the tendency for track pairs to have very similar trajectories—so similar that the tracker cannot differentiate between them. Another, and most important effect, contributing to the imperfect efficiencies is the method for determining whether certain AVHT tracks correspond to GEANT tracks. Clearly, some error is going to be made, and this error will be compounded in higher multiplicity events. The slope of the curves in Figs 3-10 and 3-11 show that the inefficiency of matching GEANT to AVHT could be up to 5% per head or tail at any multiplicity. The base-line figures seem to indicate that this estimate is a little high for heads and a little low for tails. The tracks lost due to this cut will, however, show up as spurious tracks. So in the end, the number of spurious tracks should be at least as large as the number of tracks lost due to identification inefficiencies. There are probably ways to improve the efficiencies further, but this lies in the realm of continuing research.

⁷ Note that only 4986 events (of up to 999 total active wires each) were compared, of which there were: 1659, 1873, 889, 386, 127, and 52 zero- through 5-head events, respectively, and 1238, 1535, 917, 498, 304 and 103 zero- through 5-tail events. There were some, but not many, events of higher multiplicity. Time constraints made obtaining better statistics prohibitive, though this should be done in the future.

The first cut applied to the tracks within the AVHT algorithm is the *Chi-Squared Cut*. To examine the relative effects of this cut, cuts of 2.0 and 2.85 are applied to the heads and tails, respectively, in the DST file and the resultant efficiencies are displayed in Table 4-7.

Incident Heads	Percent Found	Spurious per event		Incident Tails	Percent Found	Spurious per event
0		0.86		0		0.81
1	96.85+/-2.31	1.9		1	91.20+/-2.55	1.98
2	93.81+/-2.37	3.27		2	85.33+/-2.33	2.76
3	90.67+/-3.01	5.02		3	80.52+/-2.59	4.14
4	84.84+/-4.44	7.85		4	74.83+/-2.87	5.32
5	78.85+/-6.20	9.03		5	66.15+/-3.34	7.56

Table 4-7: Head and Tail Detection Efficiencies After the *Chi-Squared Cut*

In contrast to Table 4-6, Table 4-7 shows that while further application of the *Chi-Squared Cut* to the suggested values reduced the percentage of tracks found by about one percent, it significantly reduced the number of spurious tracks found. The increasing loss in tracks found with the number of incident particles results from the higher probability of soft electrons contributing to the high multiplicity events. These particles tend to scatter in the MWPCs and leave crooked tracks—tracks eliminated by a *Chi-Squared Cut*.

The next and final cut made by the AVHT algorithm is the *Same-Track Cut*. This cut should reveal that some of the apparently spurious tracks are really “shadows” of real tracks and which will get grouped with the real tracks. Applying this cut (2.5 for heads and 5.0 for tails) on top of the *Chi-Squared Cut* just applied, the relative efficiencies can be obtained, see Table 4-8. These cuts simulate those actually proposed for step I of the data analysis scheme of Section 4-4.

Incident Heads	Percent Found	Spurious per event		Incident Tails	Percent Found	Spurious per event
0		0.82		0		0.66
1	96.74+/-2.31	1.84		1	91.20+/-2.55	1.64
2	93.87+/-2.37	3.1		2	85.06+/-2.33	2.38
3	90.58+/-3.01	4.69		3	79.91+/-2.59	3.39
4	84.04+/-4.44	7.18		4	74.50+/-2.87	4.23
5	78.84+/-6.20	8.18		5	65.35+/-3.34	5.52

Table 4-8: Head and Tail Detection Efficiencies after the *Chi-Squared* and *Same-Track Cuts*

It is clear that the *Same-Track Cut* reduces the appearance of spurious tracks, especially in high multiplicity events, with little effect on the total percentage of tracks found correctly. The average number of spurious tracks per event is still too large.

Fortunately, according to Section 4-4, there are several ways to eliminate them. The next step involves examining all heads, identifying vertices⁸ and applying a *Source Cut* of 5.0 to those heads not contributing to vertices. This procedure results in the efficiencies shown in Table 4-9.

Incident Heads	Percent Found	Spurious per event		Incident Tails	Percent Found	Spurious per event
0		0.51		0		0.66
1	92.73+/-2.31	1.45		1	91.21+/-2.55	1.65
2	90.88+/-2.37	2.49		2	85.06+/-2.33	2.38
3	87.68+/-3.01	3.67		3	79.92+/-2.59	3.39
4	81.88+/-4.44	5.52		4	74.51+/-2.87	4.23
5	76.53+/-6.20	6.32		5	65.25+/-3.34	5.53

Table 4-9: Head and Tail Detection Efficiencies after a *Source Cut*

The *Source Cut* removes about as many spurious tracks as any other cut; however, it proves detrimental by several percent to the percentage of tracks found correctly. To see why, Figure 4-1 shows that only about 90% of the real heads actually appear to originate from the nominal collision point. Of the remaining 10%, it is surprising that even the 6.5% we are still seeing in Table 4-9 have multiple tracks passing through the detector. It is much more likely that only one of the tracks will miss and the other will be removed in a *Source Cut*. So the loss in efficiency due to this cut is really not unexpected.

Incident Heads	Percent Found	Spurious per event		Incident Tails	Percent Found	Spurious per event
0		0.25		0		0.66
1	78.11+/-2.31	1.28		1	91.21+/-2.55	1.65
2	88.41+/-2.37	2.44		2	85.06+/-2.33	2.38
3	86.87+/-3.01	3.63		3	79.92+/-2.59	3.39
4	81.69+/-4.44	5.48		4	74.51+/-2.87	4.23
5	76.53+/-6.20	6.25		5	65.25+/-3.34	5.53

Table 4-10: Head and Tail Detection Efficiencies after Removing Dangling Heads

The next step in attempting to distinguish charged and neutral particles consists of grouping the heads and tails together to form showers originating at the PbC and charged tracks passing through the entire detector. This has been implemented crudely using a

⁸ The function *stat.c:GroupTracks* can be used to make the cuts mentioned as well as determine vertices and apply the *Source Cut*, etc. The identification of vertices is made by requiring a DCA of less than 1" between the tracks as well as a nominal vertex within the box $\{(x, y, z): -100" < z < 132.65", -10" < x < 10", -5" < y < 20" \}$.

DCA cut of 1" in the region of the PbC⁹ to identify showers in combination with the probabilistic method for combining heads and tails. Once this grouping is complete, heads that do not have any tails associated with them and which do not contribute to a multiple head vertex can be removed. In practice, they are only removed if they do not point through the acceptance of the back of the detector. The results of removing these heads are displayed in Table 4-10. It is notable that this cut only affects low-occupancy events. Presumably the reason for this is that it is much less likely that heads in these events participate in a multiple track vertex. It is debatable whether these heads should actually be removed.

The final step in removing spurious tracks involves the elimination of tails that are not part of a shower or charged track and which do not point anywhere near the nominal collision point. However; since the grouping of these tracks is still crude, this cut is not analyzed here.

The preceding analysis can be refined further. In particular, the nominal collision point should be determined when possible and used in the identification of spurious heads, the nonlinear LSF should be employed to examine vertices of heads more carefully, the methods of grouping tails into showers should be refined and the electromagnetic calorimeter information should be employed to help remove spurious tails. While there is yet much work to be done both in developing the data analysis algorithms and the estimation of the errors involved, this should provide a firm basis and template for future examination.

⁹ The vertices were required to be within the 5" in z to either side of the PbC and within 9" in x-y of the center of the PbC.